2013 American Control Conference (ACC)
Washington, DC, USA, June 17-19, 2013

State of Charge Estimation of Cells in Series Connection by Using only the Total Voltage Measurement

Xinfan Lin[1], Anna G. Stefanopoulou[1], Yonghua Li[2] and R. Dyche Anderson[2]

Abstract— **The voltage of lithium ion batteries is usually monitored to prevent overcharge and overdischarge. For battery packs consisting of hundreds of cells, monitoring the voltage of every single cell adds significant cost and complexity to the battery management system (BMS). Reducing voltage sensing by only measuring the total voltage of multiple cells in series connection is desirable if the state of charge (SOC) of individual cells can be correctly estimated. Such goal cannot be achieved by an extended Kalman filter, because the cell SOCs are not observable in the linearized battery string model. In this paper, an observer based on solving simultaneously multiple nonlinear equations along the trajectory of SOC evolution is used for the estimation problem. Existence of the solution depends on the nonlinearity of the battery voltage-SOC relationship. The observer is applied to a $LiFePO_4$/graphite battery string with 2 cells, where the individual cell SOCs are observable in low and high SOC ranges. Experimental results show good convergence of SOC and voltage estimation, indicating that this new methodology can be applied to, at least, halve the voltage sensing in a battery pack.**

I. INTRODUCTION

Automotive battery systems for hybrid electric vehicles (HEV), plug-in hybrid electric vehicles (PHEV), and battery electric vehicles (BEV) usually consist of hundreds and even thousands of cells. The number of cells in a battery system is a function of the desired total voltage, power and energy, and the characteristics of the selected cell chemistry. Battery packs in HEVs with Nickel Metal Hydride (NiMH) batteries typically have 150-250 cells. Packs using lithium ion cells for the same type of vehicles have about 50-100 cells due to the higher voltage inherent to the lithium ion chemistry. Production HEVs with NiMH batteries typically measure total voltage of modules with 5 to 16 cells in series. Due to the sensitivity of most lithium ion cells to overcharge and overdischarge [1], [2], existing battery management systems (BMS) for lithium ion battery packs need to monitor the state of charge (SOC) and voltage of every single cell. This single-cell monitoring strategy adds significant cost to the lithium ion battery system including sensors, wiring and labor. Therefore, it is highly desirable to reduce the voltage sensing, e.g. by only measuring the total voltage of multiple cells, under the condition that the SOC and voltage of individual cells can still be monitored.

*This work is supported by the Ford Motor Company.

[1]X. Lin and A. Stefanopoulou are with the Department of Mechanical Engineering, University of Michigan, Ann Arbor, MI 48109, USA. Email: xflin@umich.edu and annastef@umich.edu

[2]Y. Li and R.D. Anderson are with the Vehicle and Battery Controls Department, Research and Advanced Engineering, Ford Motor Company, Dearborn, MI 48121, USA. Email: yli19@ford.com and rander34@ford.com

In this paper, the possibility of estimating the SOCs of batteries in series connection by only using the total voltage measurement is investigated. First, we try to use the extended Kalman filter (EKF), which have been widely used to estimate the battery SOC. The EKF works well when the single cell voltage is measured for feedback [3], [4], [5]. However, it has found that when only the total voltage of a battery string is measured, the EKF can only track the average SOC of the string but not the individual cell SOCs. The limitation arises from the lack of observability of the linearized battery string model discussed in Section III. In [6], the cell balancing circuit is used to augment the voltage measurement when only the total voltage is measured. In this paper, instead, it is shown that the individual cell SOCs are observable in the sense of nonlinear observability for some lithium ion battery chemistry. For example, a 2-cell string with $LiFePO_4$/graphite batteries, whose voltage-SOC relationship is highly nonlinear, is shown to have observable individual cell SOCs in low and high SOC ranges. Such nonlinear observability provides the possibility of estimating individual cell SOCs by using methods other than the EKF. The Newton observer, which is based on solving simultaneously multiple nonlinear equations along the system trajectory, [7], [8], has been proposed to address the state estimation problem with high nonlinearity. In this paper, a similar observer based on the Levenberg-Marquardt algorithm [9], [10] is designed for individual cell SOC and voltage estimation under reduced voltage sensing. Experiments under a constant charging current have been conducted to validate the proposed algorithm with a 2-cell battery string. It is demonstrated that good convergence of SOC and voltage estimation can be achieved in the high SOC range, where monitoring overcharge is of critical importance.

II. GENERALIZED BATTERY MODEL FORMULATION

Some of the most commonly used control-oriented battery models can be generalized in a state-space representation [11], as

$$\begin{aligned} \dot{x} &= Ax + BI \\ V &= g(x, I), \end{aligned} \tag{1}$$

where the state matrix A depends on the transient dynamics associated with particle diffusion [3], B on the battery capacity, and g is the nonlinear voltage output function. The state(s) x relates to the energy storage level, the input I is the current and the output V is the voltage. Such models include and are not limited to:

- Coulomb counting model (CCM) [12], [13]

- Equivalent circuit model (ECM) [13], [14]
- Simplified electrochemical model featuring lithium ion transport and diffusion during battery charge and discharge (SECM) [3], [15].

Physical meaning of the variables and parameters in (1) for the above three models are summarized in Table I. More details on the model generalization can be found in [11]. It is noted that there are more complicated partial differential equation (PDE) based battery models, which capture detailed electrochemical processes during the battery operation [16], [17]. These models may not be written in the form of (1) with linear state equations and a nonlinear output equation.

For a battery string connected in series, the current input is the same for each cell, and the measured output, the total voltage, is the summation of all the single cell voltages. In this paper, we consider the situation that the cells may only differ in their SOCs, and all the cells have the same model parameters. Such imbalance can be caused by factors such as difference among cells in self-discharge rate, which is typically related to the temperature variability along the string. Indeed, since the battery degradation is also temperature-dependent, this variability may also result in imbalance in capacity and resistance among cells. Such imbalance is more likely to be developed over longer time-span and will be addressed in the future work.

Based on the single cell model in (1), a string with r cells in series can be modeled as,

$$\begin{aligned} \dot{x}_{str} &= F(x_{str,I}) = A_{str}x_{str} + B_{str}I \\ V_{str} &= G(x_{str}, I) = \sum_{i=1}^{r} g(x_i, I), \end{aligned} \tag{2}$$

where

$$\begin{gathered} x_{str} = \begin{bmatrix} x_1 & \cdots & x_r \end{bmatrix}^T, \\ A_{str} = diag(A, \cdots, A), \quad B_{str} = \begin{bmatrix} B^T & B^T & \cdots & B^T \end{bmatrix}^T. \end{gathered} \tag{3}$$

This general form will be used in the analysis in the subsequent sections. The state estimation of (1), where the single cell voltage is measured, is referred to as the estimation under full voltage sensing, and the state estimation of (2), where only the total voltage is measured, is called the estimation under reduced voltage sensing.

III. Extended Kalman Filter and Observability of the Linearized Battery String Model

The extended Kalman filter is one of the most commonly used methods for nonlinear state estimation problems, and has been widely adopted to estimate the battery SOC under full voltage sensing [3], [4], [5]. However, it is shown here that the EKF cannot be used under reduced sensing because the linearized battery string model is not observable.

The EKF for (1) takes the form

$$\begin{aligned} \dot{\hat{x}} &= A\hat{x} + Bu + K(V - \hat{V}) \\ \hat{V} &= g(\hat{x}, I), \end{aligned} \tag{4}$$

where $\hat{x}$ and $\hat{V}$ are the estimated state(s), e.g. SOC, and voltage, V is the measured voltage and K is the observer gain. The estimated state of the EKF will converge to the real state asymptotically, if the linearized system model is observable along the system trajectory [18]. Furthermore, the linear observability practically guarantees that the errors in SOC estimation by the EKF will be bounded by some constant value even if the model parameters are not precise [11]. Such observability condition is satisfied if the single cell voltage is measured, leading to the popularity of EKF under full voltage sensing.

When only the total voltage of the string is measured, the linearized battery string model can be obtained by linearizing the output voltage function g of each single cell, as

$$g(x_i, I) = C_i x + D_i I. \tag{5}$$

As listed in Table I, C is mainly the slope of the open circuit voltage (OCV) curve and D is the ohmic resistance. Since g is a nonlinear function of the state, the values of C and D can be different for cells with different SOCs. Hence, the linearized battery string model will be

$$\begin{aligned} \dot{x}_{str} &= A_{str}x + B_{str}I \\ V_{str} &= C_{str}x + D_{str}I \\ C_{str} &= \begin{bmatrix} C_1 & C_2 & \cdots & C_r \end{bmatrix} \\ D_{str} &= \sum_{i=1}^{r} D_i, \end{aligned} \tag{6}$$

with $C_i \neq C_j$ and $D_i \neq D_j$ if $SOC_i \neq SOC_j$. The model is observable if and only if its observability matrix

$$U = \begin{bmatrix} C_{str} \\ C_{str}A_{str} \\ \cdots \\ C_{str}A_{str}^{n-1} \end{bmatrix} = \begin{bmatrix} C_1 & C_2 & \cdots & C_r \\ C_1A & C_2A & \cdots & C_rA \\ & \cdots & & \\ C_1A^{n-1} & C_2A^{n-1} & \cdots & C_rA^{n-1} \end{bmatrix} \tag{7}$$
$$\underbrace{\qquad}_{U_1} \quad \underbrace{\qquad}_{U_2} \quad \underbrace{\qquad}_{U_r}$$

is of full rank [18], [19], where n is the dimension of the A_{str} matrix. According to Tab.I, for the coulomb counting and the simplified electrochemical models, C_is are proportional to each other since they only have one non-zero element,

$$C_j = \eta_{i,j}C_i, \tag{8}$$

where $\eta_{i,j} = \frac{\alpha_j}{\alpha_i}$ for CCM, and $\eta_{i,j} = \frac{\alpha_j + \beta_j}{\alpha_i + \beta_j}$ for SECM. Hence the U_i's in (7) is linearly dependent on each other,

$$\begin{aligned} U_j &= \begin{bmatrix} C_j \\ C_jA \\ \cdots \\ C_jA^{n-1} \end{bmatrix} = \begin{bmatrix} \eta_{i,j}C_i \\ \eta_{i,j}C_iA \\ \cdots \\ \eta_{i,j}C_iA^{n-1} \end{bmatrix} = \eta_{i,j} \begin{bmatrix} C_i \\ C_iA \\ \cdots \\ C_iA^{n-1} \end{bmatrix} \\ &= \eta_{i,j}U_i. \end{aligned} \tag{9}$$

As a result, the observability matrix will be short of full rank, indicating the the linearized battery string model is unobservable. The same conclusion can be drawn for the equivalent circuit model upon similar analysis.

Simulation has been conducted to show the inadequacy of the EKF for the estimation problem under reduced voltage sensing. A coulomb counting model of the $LiFePO_4$/graphite

TABLE I

MODEL GENERALIZATION

	Coulomb counting model (CCM)	Equivalent circuit model (ECM)	Simplified electrochemical model (SECM)
State x	SOC	SOC, RC voltages: $V_{c,1}\cdots V_{c,m}$	spatially distributed lithium concentrations $c_{s,1}\cdots c_{s,q}$
Input u	current I	current I	current I
Output y	voltage V	voltage V	voltage V
A	0	$\begin{bmatrix} 0 & 0 & \cdots \\ 0 & \frac{-1}{R_{c,1}C_{c,1}} & \cdots \\ & \cdots & \\ 0 & \cdots & \frac{-1}{R_{c,m}C_{c,m}} \end{bmatrix}$ $R_{c,i}$: equivalent resistance $C_{c,i}$: equivalent capacitance	$\frac{D_s}{\Delta_r^2}\begin{bmatrix} -2 & 2 & 0 & \cdots \\ \frac{1}{2} & -2 & \frac{3}{2} & \cdots \\ & & \ddots & \\ 0 & 0 & \cdots & 0 \\ 0 & \cdots & \frac{q-1}{q} & -\frac{q-1}{q} \end{bmatrix}$ D_s: diffusion coefficient Δ_r: spatial discretization parameter
B	Q^{-1} Q: battery capacity	Q^{-1} $C_{c,i}^{-1}$	$(A_e\delta F a_s \Delta_r)^{-1}[0,\cdots,0,\frac{q+1}{q}]^T$ A_e:electrode area, δ: electrode thickness, F: Faraday constant, a_s: active particle surface
g	$OCV(SOC)+IR$, OCV: open circuit voltage R: internal resistance	$OCV(SOC)-\Sigma_i^m V_{c,i}+IR$	$OCV(c_{s,q})+OP(c_{s,q},I)+IR_f$ OP: over potential R_f: ohmic resistance
C	α α: local slope of OCV w.r.t. SOC	$\begin{bmatrix}\alpha & -1 & -1 & \cdots & -1\end{bmatrix}$	$\begin{bmatrix}0 & \cdots & 0 & \alpha+\beta\end{bmatrix}$ β: local slope of OP w.r.t. SOC
D	R	R	$R_f+\gamma$ γ: local slope of OP w.r.t. I

battery is used to emulate a battery string with 2 cells. The output voltage function of the $LiFePO_4$/graphite battery under a constant current is shown in Fig. 1. In simulation,

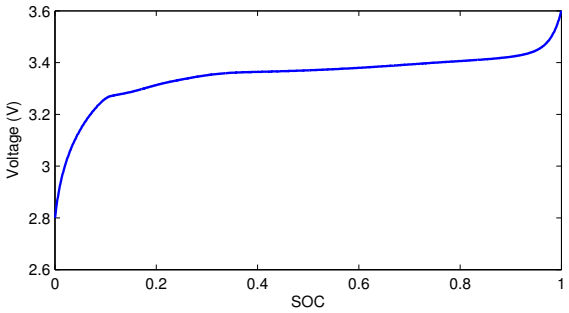

Fig. 1. Voltage-SOC relationship of $LiFePO_4$ batteries under a constant charging current

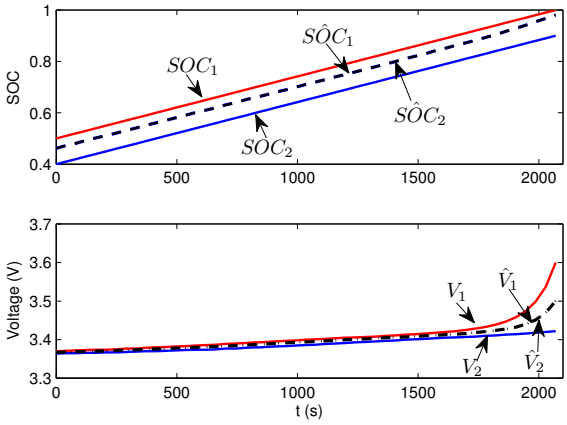

Fig. 2. Estimation of single cell SOC and string voltage by the EKF

one cell is initialized to 50% SOC, and the other to 40%. The two cells are charged with the constant current until the cell with higher SOC reaches 100% SOC mark. The total voltage of the two cells is fed back to the extended Kalman filter. Simulation results are shown in Fig. 2. It can be seen that as the two batteries are charged up, their SOCs increase linearly with time and the difference between them stays at 10%. The two estimated SOCs, however, instead of tracing SOC_1 and SOC_2 respectively, both converge to the intermediate values that would make the estimated voltage match the average voltage of the string.

IV. OBSERVABILITY ANALYSIS OF THE NONLINEAR BATTERY STRING MODEL

Although the unobservable linearized battery string model prevents the EKF from estimating the individual cell SOCs under reduced voltage sensing, it does not rule out the possibility of solving the estimation problem with a nonlinear estimation technique. The existence of the solution depends on the observability of the nonlinear battery model, which is to be investigated in this section.

A nonlinear system is observable at a certain state if the gradient (matrix) of the Lie derivative vector of the output function is of full rank [20]. For the string model in (2), the ith order Lie derivative of the output function G is

$$L_F^i(G) = V_{str}^{(i)} = \frac{\partial G}{\partial x_{str}} F(x_{str}, I), \tag{10}$$

where the current I is fixed at a constant value [20]. The Lie derivative vector is defined as

$$l(x_{str}) = \begin{bmatrix} L_F^0(G) \\ \cdots \\ L_F^{n-1}(G) \end{bmatrix}, \tag{11}$$

and the gradient of $l(x_{str})$ takes the form

$$dl(x_{str}) = \frac{\partial l}{\partial x_{str}} = \begin{bmatrix} \frac{\partial L_F^0(G)}{\partial x_{str}} \\ \cdots \\ \frac{\partial L_F^{n-1}(G)}{\partial x_{str}} \end{bmatrix}. \tag{12}$$

Consider the coulomb counting model as an example to analyze the model observability, whose $dl(x_{str})$ matrix is

$$dl(x_{str}) = \begin{bmatrix} \frac{\partial g}{\partial x}\big|_{x_1} & \cdots & \frac{\partial g}{\partial x}\big|_{x_r} \\ \frac{\partial^2 g}{\partial x^2}\big|_{x_1}\frac{I}{Q} & \cdots & \frac{\partial^2 g}{\partial x^2}\big|_{x_r}\frac{I}{Q} \\ & \cdots & \\ \frac{\partial^r g}{\partial x^r}\big|_{x_1}(\frac{I}{Q})^{n-1} & \cdots & \frac{\partial^r g}{\partial x^r}\big|_{x_r}(\frac{I}{Q})^{n-1} \end{bmatrix}, \tag{13}$$

with x_i being the SOC of the ith cell in the string. It can be seen that the rank of (13) depends on the gradients of g with respect to the SOC. Clearly, if g is linear, all its gradients higher than 2nd order will be zero, and the rank of (13) will be 1. The system will thus be unobservable under reduced voltage sensing. Nevertheless, it is possible to have a full-rank matrix in (13) if the voltage-SOC relationship g is nonlinear. For example, the $g(x)$ function of the $LiFePO_4$/graphite battery, is shown in Fig. 1 and its gradients in Fig. 3. In the SOC range between 10% and 90%, $g(x)$ is

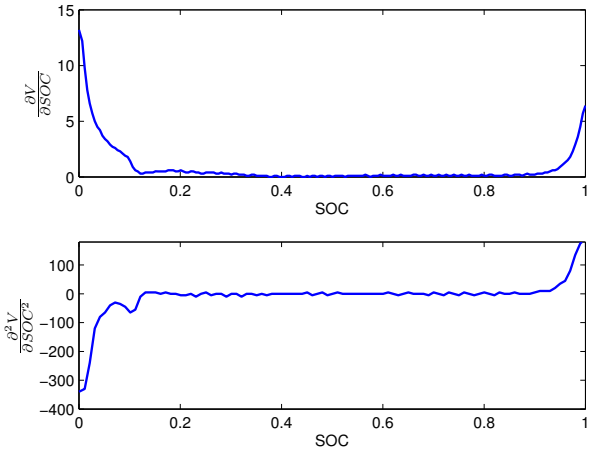

Fig. 3. Gradients of $g(x)$ for $LiFePO_4$/graphite batteries under a constant charging current

close to linear, making the battery string model unobservable. However, in the low $(0-10\%)$ and high $(90-100\%)$ SOC ranges, as shown in Fig. 1 and Fig. 3, $g(x)$ is highly nonlinear with non-zero 1st and 2nd (and even higher) order gradients. It can be checked numerically that for battery strings with two cells, the dl matrix is of full rank for any combination of individual cell SOCs along the SOC evolution trajectory. Therefore, it is possible to distinguish the individual cell SOCs when they are in those ranges. In general cases, for strings with r cells, up to $(r-1)th$ order derivatives need to be calculated to determine the rank of (13) and hence the observability. Based on the above conclusion, a nonlinear observer will be designed to estimate individual cell SOCs in a 2-cell battery string, while the methodology is applicable to strings with more cells.

V. Nonlinear Observer based on the Levenberg-Marquardt Algorithm

Apart from extending the linear estimation theory, e.g. EKF, nonlinear observers can also be constructed based on solving multiple nonlinear equations along the system evolution trajectory, such as the newton observer [7], [8]. Such algorithms, instead of handling the output data one point at a time, process the output trajectory over a certain time span simultaneously. As a result, compared with methods extended from the linear estimation theory based on model linearization, they retain the nonlinearity of the system and have a wider range of application.

Since the nonlinear observer is intended for onboard BMS, it will be designed in discrete-time domain to accommodate sampled measurements. In discrete-time domain, the model in (2) can be written as

$$\begin{aligned} x_{str,k+1} &= F_d(x_{str,k}, I_k) \\ V_{str,k} &= G(x_{str,k}, I_k), \end{aligned} \tag{14}$$

where k is the time step. The function F_d is the state equations in discrete-time domain, as

$$\begin{aligned} F_d(x_{str,k}, I_k) &= A_{str,d}x_{str,k} + B_{str,d}I_k \\ A_{str,d} = e^{A_{str}T}, \quad B_{str,d} &= \int_0^T e^{A_{str}\tau}B_{str}d\tau, \end{aligned} \tag{15}$$

where T is the sampling period.

At each estimation step, a set of N consecutive measurements and inputs,

$$V_{str,[k-N+1,k]} = \begin{bmatrix} V_{str,k-N+1} \\ \cdots \\ V_{str,k} \end{bmatrix}, I_{[k-N+1,k]} = \begin{bmatrix} I_{k-N+1} \\ \cdots \\ I_k \end{bmatrix}, \tag{16}$$

are used for estimation. Let us define

$$F_d^{I_{k+1}} \circ F_d^{I_k}(x_{str,k}) := F_d\big(F_d(x_{str,k}, I_k), I_{k+1}\big), \tag{17}$$

as $\circ$ stands for function composition. It can be derived from (14) that

$$\begin{aligned} V_{str,[k-N+1,k]} &= \begin{bmatrix} G^{I_{k-N+1}}(x_{str,k-N+1}) \\ G^{I_{k-N+2}} \circ F_d^{I_{k-N+1}}(x_{str,k-N+1}) \\ \cdots \\ G^{I_k} \circ F_d^{I_{k-1}} \circ \cdots \circ F_d^{I_{k-N+1}}(x_{str,k-N+1}) \end{bmatrix} \\ &= H(x_{str,k-N+1}, I_{[k-N+1,k]}). \end{aligned} \tag{18}$$

The problem is then reduced to solving (18) for $x_{str,k-N+1}$ given $V_{str,[k-N+1,k]}$ and $I_{str,[k-N+1,k]}$. Evolution of the state can then be determined based on (14).

The Newton observer has been proposed in [7] and [8] to solve (18). At each estimation step, $x_{str,k-N+1}$ is calculated through multiple iterations based on the Newton Raphson algorithm,

$$\begin{aligned} \tilde{x}^{j+1}_{str,k-N+1} = \tilde{x}^{j}_{str,k-N+1} &+ \left[\frac{\partial H}{\partial x_{str,k-N+1}}(\tilde{x}^{j}_{str,k-N+1}, I_{[k-N+1,k]})\right]^{-1} \\ &\big(V_{str,[k-N+1,k]} - G(\tilde{x}^{j}_{str,k-N+1}, I_{[k-N+1,k]})\big). \end{aligned} \tag{19}$$

The resulting $\tilde{x}^d_{str,k-N+1}$ at the final iteration step d, is taken as the estimation for $x_{str,k-N+1}$, as

$$\hat{x}_{str,k-N+1} = \tilde{x}^d_{str,k-N+1}. \tag{20}$$

Estimates of the subsequent states, $\hat{x}_{str,k-N+2}, \ldots, \hat{x}_{str,k}$, can then be determined by

$$\hat{x}_{str,k-i} = F_d^{I_{k-i}} \circ \ldots \circ F_d^{I_{k-N+1}}(\hat{x}_{str,k-N+1}). \tag{21}$$

At the next estimation step, $V_{str,[k-N+1,k]}$ and $I_{[k-N+1,k]}$ will be updated by the newly acquired measurements, and the initial guess of the state estimation is determined based on the previous estimation.

Although the Newton's method usually converges fast, it might not be robust under some circumstances. For example, when the gradient of $g(x)$ is small, $\frac{\partial H}{\partial x}$ in (19) becomes ill-conditioned, making it difficult to calculate its inverse. One convenient remedy is to replace the Newton iteration in (19) with the Levenberg-Marquardt iteration [9], [10], as

$$\begin{aligned}\tilde{x}^{j+1}_{str,k-N+1} =& \tilde{x}^j_{str,k-N+1} + \left[\frac{\partial H}{\partial x_{str,k-N+1}}(\tilde{x}^j_{str,k-N+1}, I_{[k-N+1,k]}) + \right. \\ & \left. \lambda \mathbf{I}\right]^{-1}\left(V_{str,[k-N+1,k]} - G(\tilde{x}^j_{str,k-N+1}, I_{[k-N+1,k]})\right),\end{aligned} \tag{22}$$

where λ is a scalar used to lower the condition number of the inverted matrix when $\frac{\partial g}{\partial x}$ is small, and $\mathbf{I}$ is the identity matrix.

VI. EXPERIMENTAL VALIDATION

Experiments have been conducted to validate the designed nonlinear observer. Two $A123$ 26650 $LiFePO_4$/graphite batteries are used for testing. Before the experiment, the two cells were first initialized with different SOCs, around 5% and 0% respectively. The two cells were then connected in series and charged up by a single current source with a constant current of 2 A. The voltage of each single cell was monitored to prevent overcharge. The actual cell SOCs were calculated based on current integration for validation. The current was cut off when the voltage of the cell with higher SOC hit 3.6 V. The actual SOCs and voltages are shown in Fig. 4.

The nonlinear observer in (22) is used to estimate the individual cell SOCs and voltages by only using the total voltage measurement. The coulomb counting model is used for the battery string model, which is adequate under the constant current charging scenario. Estimation starts at the 2000th second, and the initial guess of the SOC is taken as the same for both cells by inverting the average measured voltage. At each estimation step, 150 seconds length of data are used, corresponding to an SOC span of 4.15%. The time interval between data points is 10 s and a total of 15 sampled data are processed at each step. The estimation results are plotted in Fig. 5 and Fig. 6. The plotted value corresponds to the last point at each estimation step. The final values are shown in Tab.(II).

It can be seen from Fig. 5 that the individual cell SOCs are not distinguishable before the 12th estimation step, when

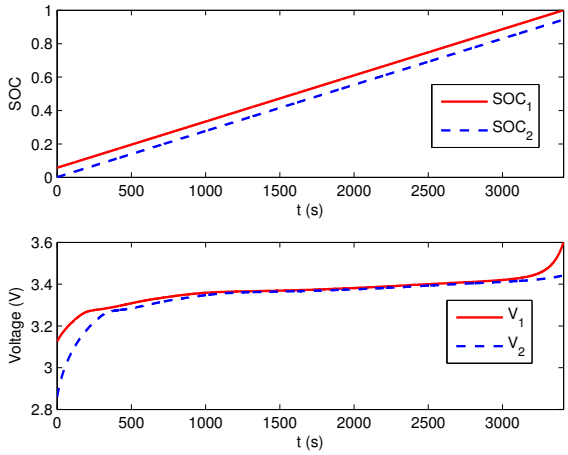

Fig. 4. Actual SOCs and voltages of individual cells

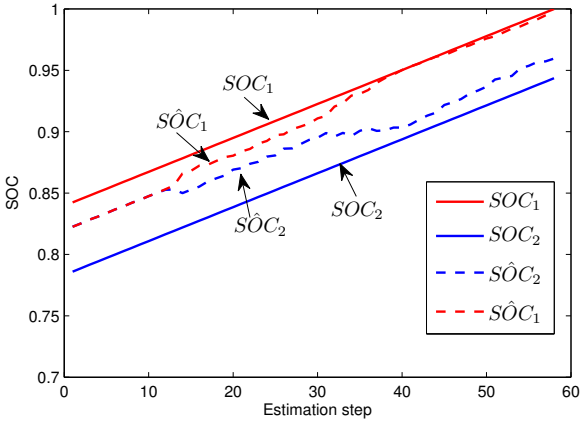

Fig. 5. SOC estimation of individual cells

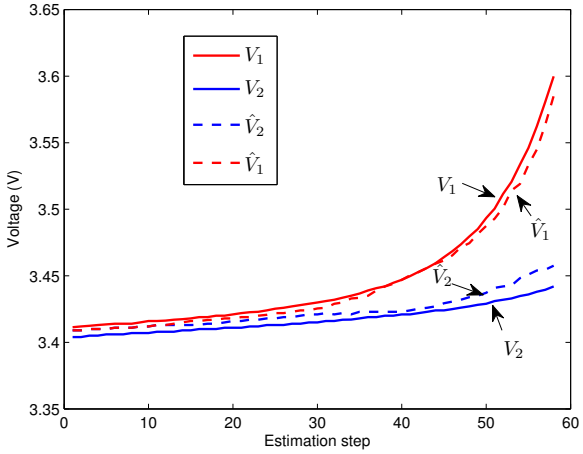

Fig. 6. Voltage estimation of individual cells

TABLE II

FINAL ESTIMATION RESULTS

	Estimation	Measurement	error (%)
SOC_1	95.99%	94.36%	1.73
SOC_2	99.81%	100%	0.19
V_1	3.46 V	3.44 V	0.58
V_2	3.59 V	3.60 V	0.28

both of them are below 85%. This has been predicted by the nonlinear observability analysis, since the model is not observable in that SOC range due to almost linear voltage-SOC relationship, as shown in Fig. 1. When the cell SOCs get above 90%, the estimates start to converge gradually to respective actual values as the model becomes observable. It can be observed that the SOC and voltage estimation of cell 1, which is the cell with the higher SOC, is more accurate than that of cell 2. The reason can be attributed to the gradients of $g(x)$ at the SOCs of the two cells. The change in total voltage can be linearized locally as

$$\delta(V_1+V_2) = \frac{\partial g}{\partial x}\Big|_{SOC_1} \delta SOC_1 + \frac{\partial g}{\partial x}\Big|_{SOC_2} \delta SOC_2. \qquad (23)$$

Since cell 1 has higher SOC, $\frac{\partial g}{\partial x}\big|_{SOC_1}$ is larger than $\frac{\partial g}{\partial x}\big|_{SOC_2}$ according to Fig. 3. Consequently, the change in total voltage will be more sensitive to the change in SOC_1. This will lead to more accurate estimation of SOC_1, which is important when the cell is nearly fully charged.

VII. CONCLUSIONS

This paper investigates the estimation of the individual cell SOCs with only the total voltage measurement for cells in series connection. It is pointed out that the existence of the solution relies on the observability of the nonlinear battery string model. For battery chemistry with linear voltage-SOC relationship, the individual cell SOCs are not observable under reduced voltage sensing. Nevertheless, for some battery chemistry, such as $LiFePO_4$, the nonlinearity of the voltage-SOC relationship renders model observability in certain SOC ranges. A nonlinear observer based on the Levenberg-Marquardt algorithm is then designed to estimate the individual cell SOCs and voltages. The algorithm has been implemented to a $LiFePO_4$/graphite battery string with 2 cells. As indicated by the observability analysis, the estimated SOCs converge faster and are much more accurate at the observable high SOC ends (than in the unobservable middle range), where the SOC estimation is more critical. In principle, the methodology can be extended to cell strings with more cells and of other chemistry given proper voltage-SOC relationship.

ACKNOWLEDGMENT

This work has been supported by the Ford Motor Company (Ford/UMICH Alliance Project) .

REFERENCES

[1] S. Hossain, Y. Saleh, and R. Loutfy, "Carbon-carbon composite as anodes for lithium-ion battery systems," *Journal of Power Sources*, vol. 96, pp. 5–13, 2001.

[2] Y.-S. Lee and M.-W. Cheng, "Intelligent control battery equalization for series connected lithium-ion battery strings," *IEEE Transactions on Industrial Electronics*, vol. 52, pp. 1297–1307, 2005.

[3] D. D. Domenico, A. Stefanopoulou, and G. Fiengo, "Lithium-ion battery state of charge and critical surface charge estimation using an electrochemical model-based extended kalman filter," *Journal of Dynamic Systems, Measurement, and Control*, vol. 132, pp. 061 302–061 313, 2010.

[4] S. Santhanagopalan and R. E. White, "Online estimation of the state of charge of a lithium ion cell," *Journal of Power Sources*, vol. 16, no. 2, pp. 1346–1355, 2006.

[5] G. L. Plett, "Extended kalman filtering for battery management systems of lipb-based hev battery packs part 3. state and parameter estimation," *Journal of Power Sources*, vol. 134, pp. 277–292, 2004.

[6] L. Y. Wang, M. Polis, G. Yin, W. Chen, Y. Fu, and C. Mi, "Battery cell identification and soc estimation using string terminal voltage measurements," *IEEE Transactions on Vehicular Technology*, vol. 61, pp. 2915–2935, 2012.

[7] P. E. Moraal and J. W. Grizzle, "Observer design for nonlinear systems with discrete-time measurements," *IEEE Transactions on Automatic Control*, vol. 40, pp. 395–404, 1995.

[8] ——, "Asymptotic observers for detectable and poorly observable systems," in *IEEE Proceedings of the 34th Conference on Decision & Control*, 1995.

[9] K. Levenberg, "A method for the solution of certain non-linear problems in least squares," *Quarterly of Applied Mathematics*, vol. 2, pp. 164–168, 1944.

[10] D. W. Marquardt, "An algorithm for least-squares estimation of non-linear parameters," *Journal of the Society for Industrial and Applied Mathematics*, vol. 11, pp. 431–441, 1963.

[11] X. Lin, A. G. Stefanopoulou, P. Laskowsky, J. S. Freudenberg, Y. Li, and R. D. Anderson, "State of charge estimation error due to parameter mismatch in a generalized explicit lithium ion battery model," in *Proceedings of ASME Dynamic Systems and Control Conference*, no. DSCC2011-6193, 2011, pp. 393–400.

[12] Y. Cadirci and Y. Ozkazanc, "Microcontroller-based on-line state-of-charge estimator for sealed leadcacid batteries," *Journal of Power Sources*, vol. 129, pp. 330–342, 2004.

[13] V. Johnson, A. Pesaran, and T. Sack, "Temperature-dependent battery models for high-power lithium-lon batteries," in *Proceedings of the 17th Electric Vehicle Symposium*, 2000.

[14] H. E. Perez, J. B. Siegel, X. Lin, A. G. Stefanopoulou, Y. Ding, and M. P. Castanier, "Parameterization and validation of an integrated electro-thermal lfp battery model," in *ASME Dynamic Systems and Control Conference (DSCC)*, 2012.

[15] K. A. Smith, C. D. Rahn, and C.-Y. Wang, "Model-based electrochemical estimation and constraint management for pulse operation of lithium ion batteries," *IEEE Transactions on Control Systems Technology*, vol. 18, pp. 654–663, 2010.

[16] T. F. Fuller, M. Doyle, and J. Newman, "Simulation and optimization of the dual lithium ion insertion cell," *Journal of the Electrochemical Society*, vol. 141, no. 1, pp. 1–10, January 1994.

[17] C. Y. Wang, W. B. Gu, and B. Y. Liaw, "Micro-macroscopic coupled modeling of batteries and fuel cells i. model development," *Journal of the Electrochemical Society*, vol. 145, no. 10, pp. 3407–3417, October 1998.

[18] Y. Song and J. W. Grizzle, "The extended kalman filter as a local asymptotic observable for discrete-time nonlinear systems," *Journal of Mathematical Systems, Estimations and Control*, vol. 5, pp. 59–78, 1995.

[19] R. Williams and D. Lawrence, *Linear state-space control systems*. Wiley, 2007.

[20] R. Hermann and A. J. Krener, "Nonlinear controllability and observability," *IEEE Transactions on Automatic Control*, vol. 5, pp. 728–740, 1977.